

LiClO₄ Electrolyte Solvate Structures

Wesley A. Henderson,^{*,†} Neil R. Brooks,[‡] William W. Brennessel,[‡] and Victor G. Young, Jr.[‡]

Department of Chemical Engineering & Materials Science, University of Minnesota, Minneapolis, Minnesota 55455, and X-ray Crystallographic Laboratory, Department of Chemistry, University of Minnesota, Minneapolis, Minnesota 55455

Received: June 27, 2003; In Final Form: October 22, 2003

Two crystalline phases, (monoglyme)₂:LiClO₄ and (diglyme)₂:LiClO₄, have been isolated and characterized. The former consists of contact ion pairs in which the anions have bidentate coordination to the Li⁺ cations, while the latter consists of fully solvated Li⁺ cations in which the cations and anions do not directly interact. The two structures are useful as models for solvate structures in concentrated electrolyte mixtures. In particular, the phase behavior and solvate structures of solvent–salt mixtures are informative when coupled with vibrational spectroscopic analysis of ionic association behavior in solutions.

Introduction

Electrolyte mixtures for use in electrochemical devices such as lithium batteries generally consist of a suitable salt (e.g., LiCF₃SO₃, LiPF₆, LiAsF₆, etc.) and one or more solvents.¹ Electrochemical stability limitations preclude the use of protic solvents in high voltage batteries. Rather, aprotic solvents such as carbonates and ethers are frequently employed. Despite the apparent simplicity of solvent–salt mixtures, the influence of solvate structures on physical properties such as ionic conductivity in liquid and solid polymer electrolytes remains poorly understood. This is especially true for the concentrated electrolytes used in batteries.

In dilute concentrations, electrolyte mixtures are often modeled as consisting of highly solvated “free” ions. The concentration dependence of the properties is then governed by long-range Coulombic forces as predicted by the Debye–Hückel theory. With increasing concentration, the ions begin to directly interact and ionic association may occur. At even higher concentrations, the electrolyte mixture properties may approach those of molten salts.² Crystalline solvates are known to form in concentrated solvent–lithium salt mixtures, and heat capacity data suggest that similar solvates persist in solutions.²

The electrolyte literature refers to solvate structures based upon the ionic association state of the ions. In carbonate and ether solvents, the relatively high donor numbers (DNs) but low acceptor numbers (ANs) of the solvents indicates that it is the cations which predominantly interact with the solvent.³ This cation solvation leads to salt dissolution and solvate formation. A competition will therefore exist between the solvent donor atoms and counteranions for coordination to cations. If the anions are weakly coordinating and/or the solvent is a strong donor, then the cations may be fully solvated by the solvent as “free” ions or solvent-separated ion pair (SSIP) solvates in which the anions remain uncoordinated. If, however, one or more anions remain coordinated to the cation, then contact ion pair

(CIP) or aggregate (AGG) solvates form. The anion in CIP solvates may, in turn, have monodentate or bidentate coordination to a Li⁺ cation which we denote as CIP-I and CIP-II solvates, respectively. Similarly, anions in AGG solvates may be coordinated to two or three Li⁺ cations denoted as AGG-I and AGG-II solvates, respectively.⁴ Other aggregated species are also possible. The very weak interactions between the solvent and anions in aprotic solvents often result in these solvate species being present even in dilute mixtures.

The degree of ionic association for a given cation (e.g., Li⁺) is determined by the solvent present and the counteranions (in addition to temperature and salt concentration). For the solvent, important factors include the strength of the donor atoms and their ability to approach the cations. Steric effects from the solvent molecules may also be important for packing considerations affecting the number of solvent molecules (and/or anions) within the cation’s solvation shell. For the anions, the ionic association strength (cation–anion interactions) is determined by the anion donor atoms, negative charge delocalization, and steric factors. To better understand the variation in ionic conductivity of electrolytes, one would like to determine the solvate formation in concentrated electrolyte mixtures and how such solvates vary with salt concentration.⁵ Other factors such as electrolyte vapor point lowering and low temperature operation are also solvate dependent and may dramatically affect the performance of a battery electrolyte. One effective tool for probing solvate formation is vibrational spectroscopy. Raman and IR spectroscopies have been extensively used for ionic association characterization of anions in liquid electrolytes. Data interpretation, however, is often greatly aided by crystalline solvate structural information.

Electrolytes containing lithium perchlorate, LiClO₄, have been widely examined. Often mixed solvents consisting of a high-permittivity solvent and low-viscosity solvent are used, such as propylene carbonate/monoglyme (PC/G1)–LiClO₄ and ethylene carbonate/diglyme (EC/G2)–LiClO₄.⁶ Glymes such as G1 and G2, CH₃O–(CH₂CH₂O)_{*n*}–CH₃ (*n* = 1 and 2, respectively), are frequently employed as low viscosity cosolvents in liquid electrolyte mixtures (η = 0.407 cP for G1 and 2.512 cP for PC at 25 °C).^{6a} There is evidence to suggest that the glyme multidentate ether solvents preferentially coordinate Li⁺ cations

* To whom correspondence should be addressed. Present address: ENEA, Casaccia Research Center, Via Anguillarese 301, 00060 Rome, Italy. Phone: +39-06-3048-4985. Fax: +39-06-3048-6357. E-mail: wesley.henderson@casaccia.enea.it.

[†] Department of Chemical Engineering & Materials Science.

[‡] Department of Chemistry.

over other cosolvents such as carbonates.^{6b,7} This may occur because of the multidentate nature and orientation of the oxygen donor atoms in glymes, resulting in more favorable cation coordination. We have examined the phase behavior of $(G1)_n$ -LiClO₄ and $(G2)_n$ -LiClO₄ mixtures. Single crystal structures of the CIP-II $(G1)_2$:LiClO₄ and SSIP $(G2)_2$:LiClO₄ solvates formed in these mixtures have been determined which provide direct information regarding the solvation state of the ions.

Experimental Section

Preparations were carried out in a dry room (<1% relative humidity, 22 °C). LiClO₄ (Aldrich) was dried at 110 °C under high vacuum for 24 h. Anhydrous G1 (monoglyme or 1,2-dimethoxyethane) (99.5%, Aldrich) and G2 (diglyme or 2-methoxyethyl ether) (99.5%, Aldrich) were used as received.

Single crystals of the $(G1)_2$:LiClO₄ compound were prepared in the following manner: G1 (0.904 g, 10.03 mmol) was added to LiClO₄ (0.177 g, 1.66 mmol). A clear solution resulted after heating the mixture while stirring. Colorless, block crystals separated on standing after several days to weeks. Single crystals of the $(G2)_2$:LiClO₄ compound were prepared in a similar manner by adding G2 (1.77 g, 13.21 mmol) to LiClO₄ (0.235 g, 2.21 mmol).

CAUTION: Perchlorate salts of metal complexes with organic ligands are potentially explosive.

Thermal characterization was performed using a liquid nitrogen cooled Perkin-Elmer Pyris 1 differential scanning calorimeter (DSC). Samples were heated to form homogeneous solutions and then hermetically sealed in Al pans. The pans were then stored for several days to weeks in the dry room before DSC measurements. Typically, the pans were slowly cooled (5 or 10 °C/min) from room temperature to -120 °C to fully crystallize the samples. The pans were then heated from -120 °C at a heating rate of 10 °C/min. Melting temperatures reported, T_m s, are the peak temperatures from heating scans.

Single crystals of $(G1)_2$:LiClO₄ and $(G2)_2$:LiClO₄ were placed on the tip of a 0.1 mm diameter glass capillary and mounted on a Bruker SMART system diffractometer for data collection at -100 °C. An inert atmosphere glovebag was used to prevent exposure of the crystals to moisture in the air. Data collection was carried out using Mo K α radiation (graphite monochromator). Intensity data were corrected for absorption and decay.⁸ Final cell constants were calculated from the xyz centroids of the strong reflections from the actual data collection after integration.⁹ Structures were solved using SIR97¹⁰ for $(G1)_2$:LiClO₄ and SIR92¹¹ for $(G2)_2$:LiClO₄ and refined using SHELXL-97.¹² Direct-methods solutions were calculated which provided most non-hydrogen atoms from the E-map. Full-matrix least squares/difference Fourier cycles were performed which located the remaining non-hydrogen atoms. All non-hydrogen atoms were refined with anisotropic displacement parameters. All hydrogen atoms were placed in ideal positions and refined as riding atoms with relative isotropic displacement parameters. The program PLATON¹³ was used for checking the structures.

Results and Discussion

Crystal Structure of $(G1)_2$:LiClO₄. Figure 1 shows the DSC heating thermograms of $(G1)_n$ -LiClO₄ mixtures. The thermal data agree well with previously reported phase diagrams of the G1-LiClO₄ system.^{2,14} The phase diagrams indicate that a stable $(G1)_2$:LiClO₄ ($T_m = 62$ °C) solvate forms in relatively good agreement with the T_m from the DSC thermogram ($T_m = 68$ °C). The uncoordinated crystalline G1 melts at -68 °C.

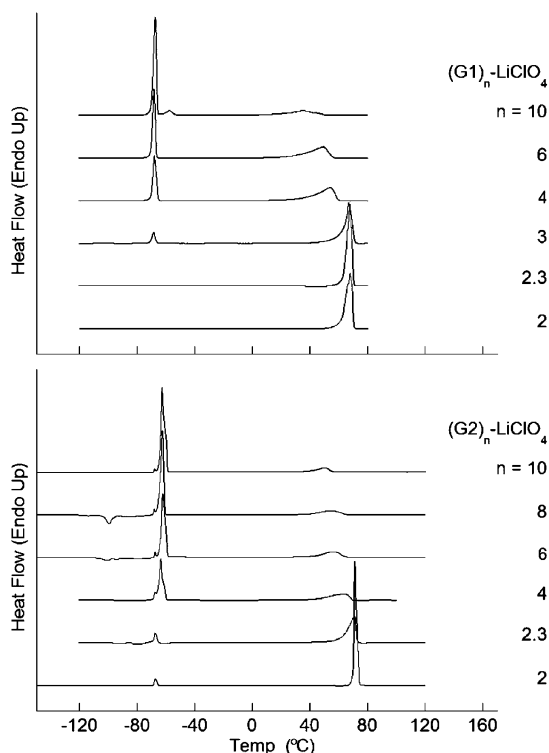


Figure 1. DSC thermograms of $(G1)_n$ -LiClO₄ and $(G2)_n$ -LiClO₄ mixtures.

TABLE 1: Crystal and Refinement Data

structure	$(G1)_2$:LiClO ₄	$(G2)_2$:LiClO ₄
chemical formula	C ₈ H ₂₀ ClLiO ₈	C ₁₂ H ₂₈ ClLiO ₁₀
fw	286.63	374.73
crystal system	monoclinic	orthorhombic
space group	C2/c	Pccn
<i>a</i> (Å)	13.147(1)	31.229(4)
<i>b</i> (Å)	8.9501(9)	12.075(2)
<i>c</i> (Å)	12.378(1)	15.127(2)
β (deg)	108.090(2)	90
<i>V</i> (Å ³)	1384.5(2)	5704.2(14)
<i>Z</i>	4	12
<i>T</i> (K)	173(2)	173(2)
ρ_{calc} (g cm ⁻³)	1.375	1.309
μ (mm ⁻¹)	0.302	0.244
crystal size (mm)	0.36 × 0.34 × 0.22	0.26 × 0.26 × 0.18
<i>F</i> (000)	608	2400
$2\theta_{\text{max}}$ (deg)	27.53	25.05
<i>N</i> (<i>R</i> _{int})	1599 (0.0275)	5048 (0.039)
<i>N</i> [<i>I</i> > 2 σ (<i>I</i>)]	1453	3672
<i>R</i> ₁ , ^a <i>wR</i> ₂ , ^b [<i>I</i> > 2 σ (<i>I</i>)]	0.0301, 0.0831	0.0400, 0.0973
<i>R</i> ₁ , ^a <i>wR</i> ₂ , ^b (all data)	0.0332, 0.1464	0.0621, 0.1133
GOFC ^c	0.993	1.023
$\Delta e_{\text{min,max}}$ (e Å ⁻³)	-0.315, 0.327	-0.532, 0.590

^a $R_1 = \sum ||F_o| - |F_c|| / \sum |F_o|$. ^b $wR_2 = [\sum [w(F_o^2 - F_c^2)^2] / \sum [w(F_o^2)^2]]^{1/2}$.
^c $\text{GOFC} = [\sum [w(F_o^2 - F_c^2)^2] / (n - p)]^{1/2}$.

Single crystal structural data for $(G1)_2$:LiClO₄ are presented in Table 1. The solvate crystal structure of $(G1)_2$:LiClO₄ consists of six-coordinate Li⁺ cations coordinated by four ether oxygen atoms from two G1 molecules and two oxygen atoms from a bidentate ClO₄⁻ anion forming isolated CIP-II [$(G1)_2$ LiClO₄] solvates (Figure 2). The coordinated G1 molecules adopt a gauche conformation which directs the uncoordinated ether oxygen lone pairs away from each other. This type of $(G1)_2$:LiX structure is common to a wide variety of simple lithium salt solvates.¹⁵

The anion Cl-O distances are listed in Table 2. The two perchlorate oxygen donor atoms coordinated to the Li⁺ cation

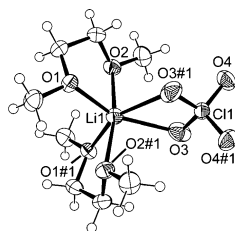


Figure 2. Coordination environment of the Li⁺ cations in (G1)₂:LiClO₄.

TABLE 2: Selected Bond Lengths (Å) and Angles (deg) for (G1)₂:LiClO₄

Li1–O1	2.028(2)	Cl1–O3	1.4429(10)
Li1–O2	2.1129(9)	Cl1–O4	1.4295(9)
Li1–O3	2.336(3)		
O1–Li1–O2	80.60(6)	O3–Li1–O2#1	95.18(8)
O1–Li1–O3	154.83(11)	O1#1–Li1–O2#1	80.60(6)
O1–Li1–O1#1 ^a	108.19(15)	O3–Cl1–O4	110.46(6)
O1–Li1–O2#1	93.14(7)	O3–Cl1–O3#1	106.11(10)
O1–Li1–O3#1	96.60(5)	O3–Cl1–O4#1	109.59(6)
O2–Li1–O3	94.05(8)	O4–Cl1–O3#1	109.59(6)
O2–Li1–O1#1	93.14(7)	O4–Cl1–O4#1	110.54(9)
O2–Li1–O2#1	169.38(17)	O3#1–Cl1–O4#1	110.46(6)
O3–Li1–O1#1	96.60(5)		

^a Symmetry transformation, #1: $-x + 1, y, -z + 1/2$.

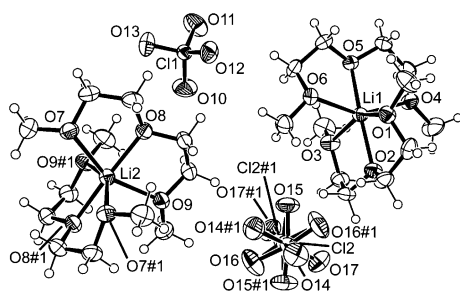


Figure 3. Coordination environment of the Li⁺ cations in (G2)₂:LiClO₄ (one anion is disordered over two positions).

have longer bonds than the uncoordinated oxygens. The Li–O distances to the perchlorate oxygen donor atoms are significantly longer than the corresponding distances to the G1 donor oxygens. The longer coordination bonds may result from the bidentate nature of the anion coordination (CIP-II). A similar structure formed with triglyme, (G3)₁:LiClO₄, has similar Li–O distances for the glyme donor oxygens, but the monodentate coordinated anion Li–O distance (CIP-I) is only 2.000 (10) Å.¹⁶

Crystal Structure of (G2)₂:LiClO₄. DSC heating thermograms of (G2)_n–LiClO₄ mixtures indicate that a stable (G2)₂:LiClO₄ ($T_m = 71$ °C) solvate forms (Figure 1). A slightly lower T_m of 66 °C has been reported for the same solvate using a DSC heating scan rate of 5 °C/min.¹⁷ The uncoordinated crystalline G2 melts at –62 °C.

Single crystal structural data for the (G2)₂:LiClO₄ phase are presented in Table 1. The solvate crystal structure of (G2)₂:LiClO₄ consists of six-coordinate Li⁺ cations coordinated by six ether oxygens from two G2 molecules (Figure 3). The anions are not coordinated to the Li⁺ cations. The ions therefore form [(G2)₂Li]⁺[ClO₄][–] SSIPs. This form of Li⁺ cation coordination has also been observed in other (G2)₂:LiX solvates.¹⁸

Although the anions are uncoordinated, the Cl–O distances are not equivalent (Table 3). Each of the two families of perchlorate anions in the unit cell contain two longer and two shorter Cl–O distances. This nonequivalence of the Cl–O bond lengths is likely due to crystalline solid-state packing effects and probably does not persist in solution even if the general

TABLE 3: Selected Bond Lengths (Å) and Angles (deg) for (G2)₂:LiClO₄

Li1–O1	2.185(4)	Cl1–O10	1.4176(17)
Li1–O2	2.111(3)	Cl1–O11	1.4161(17)
Li1–O3	2.178(4)	Cl1–O12	1.4337(16)
Li1–O4	2.132(4)	Cl1–O13	1.4319(16)
Li1–O5	2.123(3)	Cl2–O14	1.462(8)
Li1–O6	2.168(4)	Cl2–O15	1.400(16)
Li2–O7	2.240(4)	Cl2–O16	1.410(16)
Li2–O8	2.0359(14)	Cl2–O17	1.452(10)
Li2–O9	2.118(4)		
O1–Li1–O2	76.36(12)	O7–Li2–O8	75.98(9)
O1–Li1–O3	149.14(16)	O7–Li2–O9	152.16(7)
O1–Li1–O4	92.51(14)	O7–Li2–O7#1 ^a	89.3(2)
O1–Li1–O5	114.76(15)	O7–Li2–O8#1	108.94(14)
O1–Li1–O6	85.612(13)	O7–Li2–O9#1	91.379(6)
O2–Li1–O3	75.92(12)	O8–Li2–O9	77.49(10)
O2–Li1–O4	95.46(14)	O8–Li2–O7#1	108.94(14)
O2–Li1–O5	166.01(19)	O8–Li2–O8#1	173.4(3)
O2–Li1–O6	113.82(15)	O8–Li2–O9#1	98.21(13)
O3–Li1–O4	103.36(15)	O9–Li2–O7#1	91.37(6)
O3–Li1–O5	94.85(14)	O9–Li2–O8#1	98.21(13)
O3–Li1–O6	93.35(14)	O9–Li2–O9#1	100.6(2)
O4–Li1–O5	76.23(12)	O7#1–Li2–O8#1	75.98(9)
O4–Li1–O6	149.18(16)	O7#1–Li1–O9#1	152.16(7)
O5–Li1–O6	76.72(12)	O8#1–Li1–O9#1	77.49(10)
O10–Cl1–O11	110.63(13)	O14–Cl2–O15	108.0(8)
O10–Cl1–O12	109.86(11)	O14–Cl2–O16	107.6(8)
O10–Cl1–O13	108.92(11)	O14–Cl2–O17	108.1(9)
O11–Cl1–O12	109.15(11)	O15–Cl2–O16	112.3(10)
O11–Cl1–O13	109.18(12)	O15–Cl2–O17	109.9(8)
O12–Cl1–O13	109.08(10)	O16–Cl2–O17	110.7(9)

^a Symmetry transformation, #1: $-x + 1/2, -y + 1/2, z$.

forms of the Li⁺ cation solvate structures do remain in solution. The Li–O distances are all relatively short, indicating that all six of the ether oxygens have strong coordination bonds to the Li⁺ cations. Two G2 molecules, therefore, are able to pack very well around the small Li⁺ cations resulting in a high coordination number of 6.

A small endothermic peak for the (G2)₂:LiClO₄ solvate is found at –67 °C which is partially concealed by the G2 melting endothermic peaks. This suggests that a relatively minor solid–solid phase change occurs for this solvate. This may be an order–disorder transition for half of the ClO₄[–] anions in the solvate unit cell (Figure 3). Such ordering of the ClO₄[–] anions occurs in a solid–solid phase change for Ph₄PClO₄.¹⁹ The “freezing-in” of higher temperature salt disordered states on cooling has been noted by vibrational spectroscopy.²⁰ The rapid cooling of the crystals to –100 °C in the diffractometer may have frozen the observed disordered state in the crystal used for structural analysis.

Crystalline Solvates and Vibrational Spectroscopy. The ClO₄[–] and Li⁺⋯ClO₄[–] ion association interactions have been studied by ab initio calculations.²¹ Vibrational frequencies determined from such calculations may be compared with IR and Raman spectra to distinguish between various species present in electrolyte solutions. The free ClO₄[–] anion has tetrahedral symmetry (T_d) with nine vibrational degrees of freedom which are divided into four modes of vibration: ν_1 –(A₁), ν_2 –(E), ν_3 –(F₂), and ν_4 –(F₂). All of the fundamental vibrational modes are Raman active, but the degenerate modes (F₂) that are IR active appear in a region that overlaps with solvent bands.^{21a,22} For the unperturbed ClO₄[–] anion, vibrational frequencies of ν_1 (A₁) = 931 cm^{–1}, ν_2 (E) = 458 cm^{–1}, ν_3 (F₂) = 1100 cm^{–1}, and ν_4 (F₂) = 624 cm^{–1} have been reported.²³ When a polarizing Li⁺ cation (or perhaps a solvent molecule with a high AN such as H₂O) interacts with the anion, the vibrational bands are perturbed, leading to variations in the

vibrational frequencies. The ν_4 and ν_1 bands have been most frequently examined in this context.

The assignments reported for the ν_4 band are “free” ClO_4^- anions (623–626 cm^{-1}), solvated CIPs (635–639 cm^{-1}), and solvated AGGs (654–659 cm^{-1}).^{23,24} There are some discrepancies in the literature over the assignments for the ν_1 modes. James and Mayes assigned the ClO_4^- anion ν_1 vibrational bands in solvent– LiClO_4 mixtures as follows: solvated “free” ClO_4^- anions (930–934 cm^{-1}), SSIPs (938–939 cm^{-1}), solvated CIPs (944–950 cm^{-1}), and solvated AGGs (955–961 cm^{-1}).²⁵ Chabanel et al., however, noted that free anions and those in SSIPs should be spectroscopically indistinguishable.²³ The ClO_4^- anions in SSIP solvates, therefore, are not polarized to a significant enough extent to induce a shift in the vibrational band (both will have a band at 930–934 cm^{-1}). Thus, in contrast with James and Mayes, they attributed the band at 938–939 cm^{-1} to CIPs and that at 944–950 cm^{-1} to AGG dimers.

Evidence for the assignment of the 930–934 cm^{-1} ν_1 band to both “free” ClO_4^- anions and those in SSIP solvates may be found in the Raman spectrum of a SSIP poly(ethylene oxide) $\text{P(EO)}_6\text{:LiClO}_4$ crystalline phase.²⁶ A single band is observed at 932 cm^{-1} . This phase appears to be isostructural to those of the $\text{P(EO)}_6\text{:LiX}$ ($X = \text{PF}_6, \text{AsF}_6, \text{and SbF}_6$) crystalline phases²⁷ in which the five-coordinate Li^+ cations are coordinated only by polymer ether oxygens. Two PEO chains form cylinders with the Li^+ cations in the center and the uncoordinated anions arranged in rows between the cylinders. Additionally, evidence for the assignment of the 944–950 cm^{-1} ν_1 band to ClO_4^- anions coordinated to two Li^+ cations may be found in the Raman spectrum of a second AGG-I crystalline phase, $\text{P(EO)}_3\text{:LiClO}_4$.²⁶ This phase is similar to those of $\text{P(EO)}_3\text{:LiCF}_3\text{SO}_3$, $\text{P(EO)}_3\text{:LiAsF}_6$, and $\text{P(EO)}_3\text{:LiTFSI}$ in which the five-coordinate Li^+ cations are coordinated by three ether oxygens from a single PEO chain and two anion donor atoms (one each from two anions).²⁸ The same structure is found for $\text{P(EO)}_3\text{:NaClO}_4$.²⁹ The anions, in turn, are coordinated to two Li^+ cations forming solvated $[\text{Li}^+\cdots\text{ClO}_4^-]_n$ AGG-I ionic chains. The $\text{P(EO)}_3\text{:LiClO}_4$ structure is characterized predominantly by a ν_1 band at 950 cm^{-1} .²⁶

One important factor which must be considered for cation solvation is the ability of a single solvent molecule to coordinate a Li^+ cation with more than one donor atom. Multidentate solvent molecules may, in some cases, be able to pack more efficiently around the small Li^+ cations with less steric interactions than monodentate solvent molecules. Such solvents result in higher Li^+ cation coordination numbers of 5–6 and as high as 8 in 12-crown-4 $[(12\text{C}4)_2\text{Li}]^+[\text{X}]^-$ solvates (although the latter tend to have rather weak O–Li coordination bonds) rather than the coordination number of 4 typically observed for SSIPs with monodentate solvents such as THF, acetonitrile, and acetone. Glymes and PEO, $\text{CH}_3\text{O}-(\text{CH}_2\text{CH}_2\text{O})_n-\text{CH}_3$, are excellent examples as they contain multiple ether oxygens connected together by flexible ethyl segments.³⁰

IR analysis of $(\text{G}1)_n\text{-LiClO}_4$ (0.06–0.20 mol dm^{-3} at 25 °C) mixtures indicates that approximately 60–70% of the ions are SSIPs in solution. The remaining ions are CIPs.^{24c} The former are likely to be $[(\text{G}1)_3\text{Li}]^+[\text{ClO}_4^-]$ solvates which typically consist of six-coordinate Li^+ cations coordinated by six ether oxygen atoms from three G1 molecules forming SSIPs.³¹ The significant fraction of CIPs even in very dilute concentrations, however, indicates that the ClO_4^- anion competes relatively well with the G1 molecules for coordination to the cation (perhaps resulting in CIP solvates similar to $(\text{G}1)_2\text{:LiClO}_4$ in structure) (Figure 2). In contrast to $(\text{G}1)_n\text{-LiClO}_4$

mixtures, IR analysis of $(\text{G}2)_n\text{-LiClO}_4$ (0.03–0.10 mol dm^{-3} at 25 °C) mixtures indicates that approximately 90% of the ions are SSIPs in solution.^{24c} A much smaller fraction of CIPs is observed in the $(\text{G}2)_n\text{-LiClO}_4$ mixtures.

The SSIP $[(\text{G}2)_2\text{Li}]^+[\text{ClO}_4^-]$ solvate (Figure 3) is stable in the solid state, but a SSIP $[(\text{G}1)_3\text{Li}]^+[\text{ClO}_4^-]$ solvate is not. This may appear somewhat surprising since both structures are likely to contain Li^+ cations coordinated by six ether oxygens in a distorted octahedral structure. One possible explanation for this is the extra ether oxygen available in G2 molecules for tridentate coordination to the Li^+ cation relative to the bidentate coordination of G1 molecules. The Li^+ cation solvent exchange rate of the former is therefore expected to be lower than that of the latter solvent. It is also likely to be more difficult for ClO_4^- anions to replace some or all of the ether oxygens of a G2 molecule coordinated to a Li^+ cation (due to steric hindrance from the remainder of the molecule). These factors may account for the difference in solvate stability. Note that the solutions were typically allowed to equilibrate for several days to weeks at room temperature prior to thermal analysis. The high fraction of SSIPs in the $(\text{G}1)_n\text{-LiClO}_4$ solutions suggests that a SSIP $(\text{G}1)_3\text{:LiClO}_4$ crystalline solvate may form, but perhaps the T_m of this solvate is below room temperature. A small endothermic peak found near –57 °C for the $(\text{G}1)_n\text{-LiClO}_4$ ($n = 10$) sample supports this conclusion. The more thermally stable CIP $(\text{G}1)_2\text{:LiClO}_4$ solvate, however, may crystallize instead on standing at room temperature. Further analysis of cooled melts should clarify this.

Direct comparisons between known solvate structures and vibrational spectra should identify the correct assignments for the multiple anion vibrational bands observed for different solvate species with $\text{Li}^+\cdots\text{ClO}_4^-$ coordination. Vibrational spectroscopic analysis is currently in progress for the known structures of the SSIP $(\text{G}2)_2\text{:LiClO}_4$, CIP-I $(\text{G}3)_1\text{:LiClO}_4$,¹⁶ and CIP-II $(\text{G}1)_2\text{:LiClO}_4$ solvates as well as crystalline LiClO_4 .³² This, in turn, should aid in the understanding of the ionic solvation behavior in liquid or amorphous polymer electrolytes.

Conclusions

Two crystalline phases, $(\text{G}1)_2\text{:LiClO}_4$ and $(\text{G}2)_2\text{:LiClO}_4$, have been isolated and structurally characterized. The former consists of CIP-II solvates in which the Li^+ cations have bidentate coordination to a single ClO_4^- anion. The latter consists of SSIP solvates in which the Li^+ cations are not coordinated by the ClO_4^- anions. These solvate structures provide a valuable tool for the vibrational spectroscopic characterization of electrolytes.

Acknowledgment. W.A.H. is indebted to the University of Minnesota and the National Science Foundation for Graduate Research Fellowships.

Supporting Information Available: X-ray crystallographic data files for the $(\text{G}1)_2\text{:LiClO}_4$ and $(\text{G}2)_2\text{:LiClO}_4$ solvate structures (CIF). This material is available free of charge via the Internet at <http://pubs.acs.org>.

References and Notes

- (1) (a) *Handbook of Battery Materials*; Besenhard, J. O., Ed.; Wiley-VCH: New York, 1999. (b) *Handbook of Batteries*, 3rd ed.; Linden, D., Reddy, T. B., Eds.; McGraw-Hill: New York, 2002. (c) *Lithium Batteries. New Materials, Developments and Perspectives*; Pistoia, G., Ed.; Elsevier: New York, 1994.
- (2) Couture, L.; Desnoyers, J. E.; Perron, G. *Can. J. Chem.* **1996**, *74*, 153.
- (3) Gutmann, V.; Resch, G.; Linert, W. *Coord. Chem. Rev.* **1982**, *43*, 133.

- (4) Huang, W.; Frech, R.; Wheeler, R. A. *J. Phys. Chem.* **1994**, *98*, 100.
- (5) (a) Rhodes, C. P.; Frech, R. *Macromolecules* **2001**, *34*, 2660. (b) Brouillette, D.; Irish, D. E.; Taylor, N. J.; Perron, G.; Odziemkowski, M.; Desnoyers, J. E. *Phys. Chem. Chem. Phys.* **2002**, *4*, 6063.
- (6) (a) Gores, H. J.; Barthel, J. *Pure Appl. Chem.* **1995**, *67*, 919. (b) Ishikawa, M.; Wen, S.-Q.; Matsuda, Y. *J. Power Sources* **1993**, *45*, 229. (c) Geoffroy, I.; Willmann, P.; Mesfar, K.; Carré, B.; Lemordant, D. *Electrochim. Acta* **2000**, *45*, 2019.
- (7) (a) Gores, H. J.; Barthel, J. *J. Solution Chem.* **1980**, *9*, 939. (b) Morita, M.; Asai, Y.; Yoshimoto, N.; Ishikawa, M. *J. Chem. Soc., Faraday Trans.* **1998**, *94*, 3451. (c) Matsuda, Y.; Nakashima, H.; Morita, M.; Takasu, Y. *J. Electrochem. Soc.* **1981**, *128*, 2552. (d) Matsuda, Y.; Morita, M.; Tachihara, F. *Bull. Chem. Soc. Jpn.* **1986**, *59*, 1967. (e) Chintapalli, S.; Frech, R. *Solid State Ionics* **1996**, *86–88*, 341. (f) Frech, R.; Chintapalli, S. *Solid State Ionics* **1996**, *85*, 61.
- (8) Blessing, R. *Acta Crystallogr., Sect. A* **1995**, *51*, 33. Sheldrick, G. M. *SADABS*; Bruker Analytical X-Ray Systems: Madison, WI.
- (9) *SAINT*, V6.1; Bruker Analytical X-Ray Systems: Madison, WI.
- (10) Altomare, A.; Burla, M. C.; Camalli, M.; Cascarano, G.; Giacovazzo, C.; Guagliardi, A.; Moliterni, A. G. G.; Polidori, G.; Spagna, R. *SIR97. J. Appl. Crystallogr.* **1998**, *32*, 115.
- (11) Altomare, A.; Cascarano, G.; Giacovazzo, C.; Gualardi, A. *SIR92. J. Appl. Crystallogr.* **1993**, *26*, 343.
- (12) *SHELXTL*, V6.10; Bruker Analytical X-Ray Systems: Madison, WI.
- (13) Spek, A. L. *PLATON. Acta Crystallogr., Sect. A* **1990**, *46*, C34.
- (14) Perron, G.; Couture, L.; Lambert, D.; Desnoyers, J. E. *J. Electroanal. Chem.* **1993**, *355*, 277.
- (15) (a) Nichels, M. A.; Williard, P. G. *J. Am. Chem. Soc.* **1993**, *115*, 1568. (b) Palizsch, W.; Böhme, U.; Roewer, G. *Chem. Commun.* **1997**, 803. (c) Palizsch, W.; Böhme, U.; Beyer, C.; Roewer, G. *Organometallics* **1998**, *17*, 2965. (d) Palizsch, W.; Beyer, C.; Böhme, U.; Rittmeister, B.; Roewer, G. *Eur. J. Inorg. Chem.* **1999**, 1813. (e) Wetzels, T. G.; Roesky, P. *W. Organometallics* **1998**, *17*, 4009. (f) Wetzels, T. G.; Dehnen, S.; Roesky, P. *W. Organometallics* **1999**, *18*, 3835.
- (16) Henderson, W. A.; Brooks, N. R.; Brennessel, W. W.; Young, V. G., Jr. *J. Chem. Mater.* **2003**, *15*, 4679.
- (17) Grondin, J.; Ducasse, L.; Bruneel, J.-L.; Servant, L.; Lassègues, J.-C. *Solid State Ionics*, in press.
- (18) (a) Becker, G.; Eschbach, B.; Mundt, O.; Reti, M.; Niecke, E.; Issberner, K.; Nieger, M.; Thelen, V.; Nöth, H.; Waldör, R.; Schmidt, M. *Z. Anorg. Allg. Chem.* **1998**, *624*, 469. (b) Huang, W. Ph.D. Thesis. University of Oklahoma, 1994. (c) Rogers, R. D.; Bynum, R. V.; Atwood, J. L. *J. Crystallogr. Spectrosc. Res.* **1984**, *14*, 29. (d) Riffel, H.; Neumüller, B.; Fluck, E. *Z. Anorg. Allg. Chem.* **1993**, *619*, 1682. (e) Giese, H.-H.; Nöth, H.; Schwenk, H.; Thomas, S. *Eur. J. Inorg. Chem.* **1998**, 941. (f) Becker, G.; Schwarz, W.; Seidler, N.; Westerhausen, M. *Z. Anorg. Allg. Chem.* **1992**, *72*, 612.
- (19) (a) Batten, S. R.; Harris, A. R.; Murray, K. S. *Acta Crystallogr., Sect. C* **2000**, *56*, 1394. (b) Vittal, J. J.; Dean, P. A. W. *Acta Crystallogr., Sect. C* **1996**, *52*, 3185.
- (20) Naudin, C.; Bonhomme, F.; Bruneel, J. L.; Ducasse, L.; Grondin, J.; Lassègues, J. C.; Servant, L. *J. Raman Spectrosc.* **2000**, *31*, 979.
- (21) (a) Klassen, B.; Aroca, R.; Nazri, G. A. *J. Phys. Chem.* **1996**, *100*, 9334. (b) Johansson, P.; Jacobsson, P. *J. Phys. Chem. A* **2001**, *105*, 8504.
- (22) Xuan, X.; Wang, J.; Lu, J.; Pei, N.; Mo, Y. *Spectrochim. Acta, Part A* **2001**, *57*, 1555.
- (23) Chabanel, M.; Legoff, D.; Touaj, K. *J. Chem. Soc., Faraday Trans.* **1996**, *92*, 4199.
- (24) (a) Xu, M.; Inoue, N.; Eyring, E. M.; Petrucci, S. *J. Phys. Chem.* **1988**, *92*, 2789. (b) Salomon, M.; Xu, M.; Eyring, E. M.; Petrucci, S. *J. Phys. Chem.* **1994**, *98*, 8234. (c) Firman, P.; Xu, M.; Eyring, E. M.; Petrucci, S. *J. Phys. Chem.* **1993**, *97*, 3606. (d) Maaser, H.; Xu, M.; Hemmes, P.; Petrucci, S. *J. Phys. Chem.* **1987**, *91*, 3047.
- (25) (a) James, D. W.; Mayes, R. E. *J. Phys. Chem.* **1984**, *88*, 637. (b) James, D. W.; Mayes, R. E. *Aust. J. Chem.* **1982**, *35*, 1785. (c) James, D. W.; Mayes, R. E. *Aust. J. Chem.* **1982**, *35*, 1775.
- (26) Ducasse, L.; Dussauze, M.; Grondin, J.; Lassègues, J.-C.; Naudin, C.; Servant, L. *Phys. Chem. Chem. Phys.* **2003**, *5*, 567.
- (27) (a) Robitaille, C. D.; Fauteux, D. *J. Electrochem. Soc.* **1986**, *133*, 315. (b) MacGlashan, G. S.; Andreev, Y. G.; Bruce, P. G. *Nature* **1999**, *398*, 792. (c) Martin-Litas, I.; Andreev, Y. G.; Bruce, P. G. *Chem. Mater.* **2002**, *14*, 2166. (d) Henderson, W. A.; Passerini, S. *Electrochem. Commun.* **2003**, *5*, 575.
- (28) (a) Lightfoot, P.; Mehta, M. A.; Bruce, P. G. *Science* **1993**, *262*, 883. (b) Gadjourova, Z.; Martín y Marero, D.; Andersen, K. H.; Andreev, Y. G.; Bruce, P. G. *Chem. Mater.* **2001**, *13*, 1282. (c) Andreev, Y. G.; Lightfoot, P.; Bruce, P. G. *Chem. Commun.* **1996**, 2169.
- (29) Lightfoot, P.; Mehta, M. A.; Bruce, P. G. *J. Mater. Chem.* **1992**, *2*, 379.
- (30) (a) Müller-Plathe, F.; van Gunsteren, W. F. *J. Chem. Phys.* **1995**, *103*, 4745. (b) Borodin, O.; Smith, G. D. *Macromolecules* **1998**, *31*, 8396. (c) Johansson, P.; Tegenfeldt, J.; Lindgren, J. *Polymer* **1999**, *40*, 4399.
- (31) (a) Näther, C.; Bock, H.; Havlas, Z.; Hauck, T. *Organometallics* **1998**, *17*, 4707. (b) Bock, H.; Beck, R.; Havlas, Z.; Schödel, H. *Inorg. Chem.* **1998**, *37*, 5046. (c) John, M.; Auel, C.; Behrens, C.; Marsch, M.; Harms, K.; Bosold, F.; Gschwind, R. M.; Rajamohanam, P. R.; Boche, G. *Chem. Eur. J.* **2000**, *6*, 3060.
- (32) Henderson, W. A.; Brooks, N. R. *Inorg. Chem.* **2003**, *42*, 4522.